ISBN 86-7306-063-6

22nd SPIG CONTRIBUTED PAPERS

SPIG 2004

22nd Summer School and International Symposium on the Physics of Ionized Gases

August 23-27, 2004, National Park Tara, Bajina Bašta, Serbia and Montenegro

CONTRIBUTED PAPERS

&

ABSTRACTS of INVITED LECTURES,
TOPICAL INVITED LECTURES and PROGRESS REPORTS

Editor:
Ljupčo Hadžievski

Vinča Institute of Nuclear Sciences
Belgrade, Serbia and Montenegro

22nd Summer School and International Symposium on the Physics of Ionized Gases

SPIG 2004

CONTRIBUTED PAPERS

&

ABSTRACTS OF INVITED LECTURES, TOPICAL INVITED LECTURES and PROGRESS REPORTS

Editor
Ljupčo Hadžievski

Vinča Institute of Nuclear Sciences
Belgrade, Serbia and Montenegro

Belgrade, 2004

CONTRIBUTED PAPERS & ABSTRACTS OF INVITED LECTURES,
TOPICAL INVITED LECTURES and PROGRESS REPORTS
of the
22nd SUMMER SCHOOL AND INTERNATIONAL SYMPOSIUM
ON THE PHYSICS OF IONIZED GASES

23 - 27 August 2004
National Park Tara, Bajina Bašta, Serbia and Montenegro

Editor
Ljupčo Hadžievski

Publisher
Vinča Institute of Nuclear Sciences
P. O. Box 522
11001 Belgrade
Serbia and Montenegro

Computer processing
Zoran Ristić

Printed by
BRANMIL
Borisa Kidriča 24, Borča, Belgrade

Number of copies
300

ISBN 86-7306-063-6

PREFACE

This book contains the Contributed papers and abstracts of the Invited lectures, Topical invited lectures and Progress reports to be presented at the 22th Summer School and International Symposium on the Physics of Ionized Gases – SPIG 2004. The Symposium will be held in Tara, Bajina Bašta, Serbia and Montenegro, from August 23 to August 27, 2004. The meeting is organized by the Vinča Institute of Nuclear Sciences, Belgrade, Serbia and Montenegro under the auspices of the Ministry of Science and Environmental Protection, Republic of Serbia.

The Invited lectures and Contributed papers are related to the following research fields: Atomic Collision Processes, Particle and Laser Beam Interaction with Solids, Low Temperature Plasmas and General Plasmas. The length of Contributed papers is limited to a maximum of four pages. Each Contributed paper is supposed to present an original work with sufficient amount of scientific information.

The Editor would like to thank the members of the Scientific and Advisory Committees of SPIG 2004 for their efforts in proposing the invited lectures and progress reports, revue of the contributed papers and selection of 14 papers for the oral presentation.

The participants have been asked to send their papers camera ready, so no typing, spelling and grammatical errors have been corrected in the course of preparation of this book.

July, 2004 Ljupčo Hadžievski

SPIG 2004

SCIENTIFIC PROGRAM

SPIG 2004

INTERNATIONAL SCIENTIFIC COMMITTEE

T. Grozdanov (Chairman) SCG
N.Bibić (Vice-chairman) SCG

S. Buckman	AUS	K. Lieb	GER
M. Dimitrijević	SCG	T. Makabe	JPN
S. Djurović	SCG	G. Malović	SCG
M. Kuraica	SCG	N. Nedeljković	SCG
Lj. Hadžievski	SCG	M. Radović	SCG
J. Jureta	SCG	D. Jovanović	SCG

ADVISORY COMMITTEE

D. Belić	B. Perović
N. Konjević	Z. Petrović
J. Labat	M. Popović
B. Marinković	J. Purić
B. Milić	B. Stanić
M. Milosavljević	M. Škorić

ORGANIZING COMMITTEE

Lj. Hadžievski (Chairman)
Z. Ristić (Secretary)

B. Gaković	Lj. Nikolić
B. Marković	N. Bundaleski
Z. Marković	N. Bibić
D. Peruško	M. R. Radović

Electron-impact Excitation of the ($4f^{14}$ 6s6p) $^1P_1$ Level in Ytterbium

B Predojević[2], D Šević[1], V Pejčev[1,3], B P Marinković[1], D M Filipović[1,4]

[1]*Institute of Physics, PO Box 57, 11001, Belgrade, Serbia and Montenegro*
[2]*Faculty of Natural Sciences, University of Banja Luka, Republic of Srpska, Bosnia and Herzegovina*
[3]*Faculty of Natural Sciences, University of Kragujevac, Serbia and Montenegro*
[4]*Faculty of Physics, University of Belgrade, PO Box 368 11001, Belgrade Serbia and Montenegro*

Abstract. Differential cross sections (DCSs) for inelastic electron scattering by ytterbium atom were measured at 20 and 80 eV electrons impact energies (E_o). These measurements were performed at scattering angles (θ) between 2° and 70°. The absolute DCS scale for the 6s6p $^1P_1$ state was determined through normalization to experimental results of Johnson *et al* (1998, *J. Phys. B: At. Mol. Opt. Phys.* **31,** 3027). Our results are compared with other available experimental and theoretical data.

INTRODUCTION

The electronic structure of ytterbium makes this alkaline-earth-like atom very suitable for investigation of numerous electron-atom collision processes. Ytterbium is a heavy atom (Z=70) and can therefore provide a testing ground for the importance of relativistic effects in electron-atom scattering. Electron-impact excitation of ytterbium is of practical importance because ytterbium vapour has potential suitability as a laser medium (Klimkin 1975). Moreover, Takasu *et al* (2003) found that optically trapped Yb atoms can have important application, especially in fundamental physics as a test of time-reversal symmetry and parity violation.

Previous experimental results of electron scattering by ytterbium have been presented by Shimon *et al* (1981), Kazakov and Hristoforov (1983), Mandy *et al* (1993), Johnson *et al* (1998) and Zetner *et al* (2001). The available theoretical calculations of differential cross section (DCSs) are restricted to the distorted-wave approximation (DW). Relativistic DW was used by Srivastava *et al* (1995), and unitarized DW by both Johnson *et al* (1998) and Zetner *et al* (2001).

EXPERIMENTAL PROCEDURE

The apparatus used for the measurements is a conventional cross-beam electron spectrometer described elsewhere (Predojević *et al* 2003). The spectrometer operates in energy-loss (ΔE) mode. The metal-vapour beam source has been described in detail by Tošić *et al* (2003). Overall energy resolution (as FWHM) is about 65 meV. The angular resolution of the spectrometer is estimated to be 1.5°. The impact energy scale

was calibrated by measuring the position of the feature in the elastic scattering attributed to the threshold energy of the 5 ^{3}P excitation of Cd at 3,737 eV (Marinković *et al* (1991)).

The measurements were performed at temperature of 870 K for ytterbium of 99.99% purity. Working temperature correspond to the metal-vapor pressure of approximately 5.2 Pa. The Yb vapour effuses through a cylindrical channel in the cap with aspect ratio γ=0.075.

Relative DCSs are obtained as follows. For an impact energy (E_0) and a given (ΔE), position of the analyzer was changed from 0° to 70° and the angular distribution of scattered electrons was measured. A correction of the intensity distribution was made due to an angular dependence of the effective interaction volume. The effective path-length correction factors (F) (Brinkman and Trajmar 1981) were calculated using procedure described by Marinković *et al* (1991) for Cd. The relative DCSs were normalized at scattering angle θ = 10° using the absolute DCSs measured by Johnson *et al* (1998). Also, energy-loss spectra at other scattering angles were recorded.

RESULTS AND DISCUSSION

An energy-loss spectrum at 20 eV impact energy and scattering angle 10° is shown in figure 1. The 6s6p ^{3}P$_1$, 6s6p^{1}P$_1$, 5d6s ^{1}D$_2$ and (7/2, 5/2)$_1$° features are clearly resolved with resolution mentioned above. Contribution of the 5d6s ^{3}D$_{1,2,3}$ excitation to the 6s6p ^{1}P$_1$ feature is also possible.

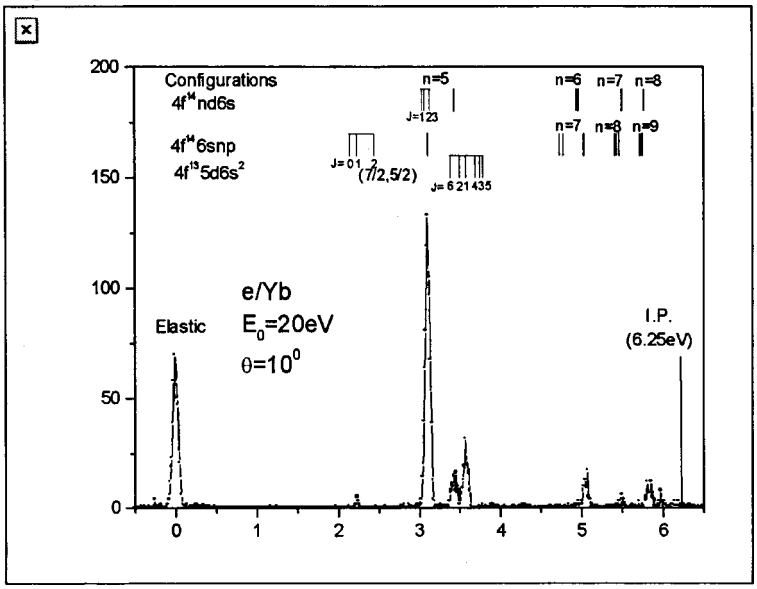

FIGURE 1. Electron energy-loss spectrum of Yb atom at E_o =20eV impact energy and θ = 10° scattering angle.

Our experimental DCSs of the 6s6p $^1P_1$ level are presented in figure 2. The theoretical RDW and UDW calculations and previous experimental results (Johnson *et al* (1998)) are also shown.

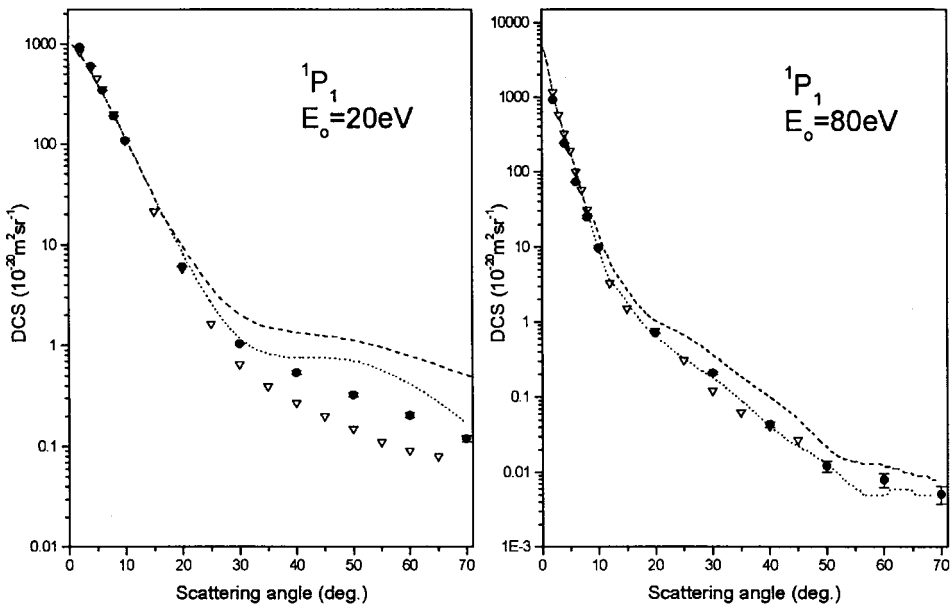

FIGURE 2. Differential cross section for excitation of the 6s6p $^1P_1$ level at 20eV and 80eV impact energies. Experiments: •, present (statistical error bars are indicated); ∇, Johnson *et al* (1988). Calculations: ···, UDW Johnson *et al* (1998); ——, RDW Srivastava *at al* (1995).

At 20 eV impact energy and scattering angles $\theta < 10^\circ$ our results are in good agreement with both previous calculations and measurements by Johnson *et al* (1998). At scattering angles $\theta > 10^\circ$ situation becomes less satisfactory. In this range of scattering angles our DCSs are placed between the theoretical and experimental results. At 80eV impact energy agreement between our measurements, results of Johnson *et al* and UDW are very good. Generally, RDW theory overestimates differential cross section, with better agreement at higher impact energies.

ACKNOWLEDGMENTS

This work has been done under project IO1424 financed by MNZŽS of the Republic of Serbia.

REFERENCES

1. Brinkman, R. T., and Trajmar, S., *J. Phys. E: Sci. Instrum.* **14,** 245 (1981).
2. Johnson, P. V., Li, Y., Zetner, P. W., Csanak, G., Clark, R. E., and Abdallah, J., *J. Phys. B: At. Mol. Opt. Phys.* **31,** 3027 (1998).
3. Kazakov, S. M., and Hristoforov, O. V., *Opt. Spektrosk.* **54,** 750 (1983).
4. Klimkin, V. G., *Sov. J. Quantum Electron.* **5,** 326 (1975).
5. Mandy, J. A., Romanyuk, M. I., Papp, F. F., Shpenik, O. B., *Proc. 18th Int. Conf. On the Physics of Electronic and Atomic Collisions (Aarhus)* ed. Andersen, T., Fastrup, B., Folkmann F., and Knudsen, H., (Bristol: Hilger) (1993) Abstracts p. 167.
6. Marinković, B., Pejčev, V., Filipović, D., and Vušković, L., *J. Phys. B: At. Mol. Opt. Phys.* **24,** 1817 (1991).
7. Predojević, B., Šević, D., B., Pejčev, V., Marinković, B., and Filipović, D., *J. Phys. B: At. Mol. Opt. Phys.* **36,** 2371 (2003).
8. Shimon, L. L., Golovchak, N. V., Garga, I. I., and Kurta, I. V., *Opt. Spektrosk.* **50,** 1037 (1981).
9. Srivastava, R., McEachran, R. P., and Stauffer, A. D., *J. Phys. B: At. Mol. Opt. Phys.* **28,** 885 (1995).
10. Takasu, Y., Honda, K., Komori, K., Kumakura, M., Takahashi, Y., and Yabuzaki, T., *Phys. Rev. Lett.* **90,** 023003 (2003).
11. Tošić, S., Šević, D., Pejčev, V., Filipović, D., and Marinković, B. P., *Fifth General Conference of the Balkan Physical Union (Vrnjačka Banja),* ed. Jokić, S., Milošcvić, I., Balaž, A., Nikolić, Z., (Belgrade) Abstracts p 54.
12. Zetner, P. W., Johnson, P. V., Li, Y., Csanak, G., Clark, R. E., and Abdalah, J., *J. Phys. B: At. Mol. Opt. Phys.* **34,** 1619 (2001).

Elastic Electron Scattering by Tetrahydrofuran

A. R. Milosavljević[1], A. Giuliani[2], M.-J. Hubin-Franskin[2] and B. P. Marinković[1]

[1]*Institute of Physics, P. O. Box 57, 11001 Belgrade, Serbia and Montenegro*
[2]*Laboratoire de Spectroscopie d'Electrons Diffusés, Université de Liège, Institut de Chimie, Bâtiment B6c, B-4000 Liège, Belgium*

Abstract. We report preliminary results for elastic and inelastic scattering below 0.5 eV of energy loss, of electrons by gaseous tetrahydrofuran (C_4H_8O), which is the DNA backbone sugar-like analogue molecule. The relative elastic differential cross section (DCS) as a function of scattering angle (10°-110°) is presented at 30 eV impact electron energy. Also, the contribution of near zero vibrational excitation to the overall energy loss signal from 0 eV to 0.45 eV was investigated as a function of scattering angle.

INTRODUCTION

The monomer units of DNA molecule (nucleotides) consist of a 5-carbon sugar (deoxyribose), a nitrogen containing base attached to the sugar and a phosphate group. However, the backbone of the DNA molecule may be seen as a series of tetrahydrofuran (THF) molecules connected by phosphate bonds to which the bases are attached (figure 1). In recent years, it has been emphasized the importance of investigation of electron interaction with molecules whose basic features approximate those found in the deoxyribose backbone of DNA [1, 2]. This could contribute to qualitative estimation of effects linked to chemical and structural changes of cellular DNA connected with radiation damage. To date, there are no data of angular and energy dependence of DCS for electrons elastically scattered by THF. In addition, we investigate the contribution of inelastically scattered electrons to the overall energy loss signal in the range 0 eV to 0.45 eV, as a function of scattering angle. The high-resolution electron energy loss vibrational data of THF for this energy region have been reported recently [1].

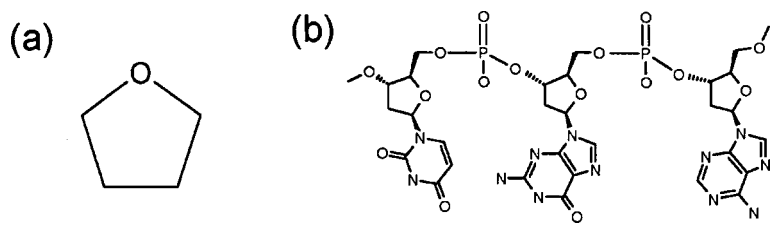

FIGURE 1. Schematic drawing of (a) tetrahydrofuran molecule and (b) short-chain segment of a single-stranded backbone of DNA.

EXPERIMENTAL SETUP

The VG-SEELS 400 electron energy loss spectrometer has been described in detail elsewhere [3]. In short, it consists of an electron gun followed by monochromator, electron energy analyzer and channel electron multiplier as a detector. Both monochromator and analyzer are 150° hemispherical electrostatic type and are fitted with three aperture electrostatic zoom lenses. The effusive molecular beam is formed using the stainless steal needle placed perpendicularly to the incident electron beam. The analyzer can be rotated around the molecular beam in the range −10° to +110°. The angular resolution was investigated earlier [4] and was found to be better than ±2°. The energy loss spectra have been recorded in the constant pass energy mode, with the pass energy of 4 eV and with 8 meV steps. The overall energy resolution was about 45 meV, as measured at the FWHM of the elastic peak. During the acquisition, the retarding and focusing potentials of the analyzer were controlled by the computer. The operating pressure was 1.3×10^{-5} mbar and the base pressure was better than 1.0×10^{-8} mbar (obtained by cryogenic pumping). For each measurement, the incident beam current was monitored using a Faraday cup. Also, the influence of the effective path length correction was obtained according to elastic DCS for nitrogen, which was measured under the same experimental conditions and compared to existing data [5].

RESULTS AND DISCUSSION

Electron energy loss spectra

A typical electron energy loss spectrum of THF in the region up to 0.45 eV, at the scattering angle of 30° and for impact electron energy of 30 eV is presented in figure 2. The strong elastic peak near zero energy loss possess a slight asymmetry, which is due to the excitation of rotational and vibrational levels that can not be resolved. Some structures in the inelastic part of the spectrum are believed to originate from vibrational excitations and are investigated in detail elsewhere [1].

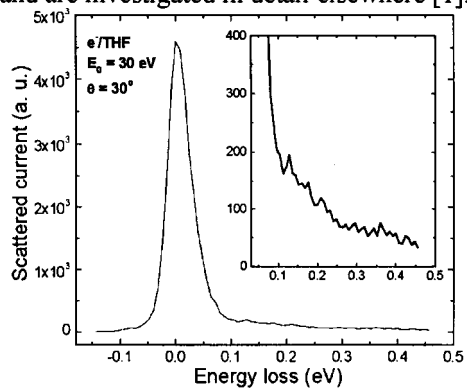

FIGURE 2. Electron energy loss specter of THF recorded at 30 eV and 30° .

Elastic DCS

The relative differential cross section for elastic electron scattering by THF, for 30 eV impact electron energy, is presented in figure 3a. For each scattering angle, the relative DCS was obtained by both integrating the whole quasielastic energy loss peak (up to 0.45 eV) and only by integrating the low-energy part (up to 0 eV). The DCS descends rapidly up to about 90° with the increase of scattering angle. Also, one can see the existence of the minimum at about 90°. Since there are no published data for elastic electron scattering by THF, we can not compare present results with previous ones. However, there is similarity with the behavior of elastic DCS for some other molecular targets at 30 eV impact energy [3, 4].

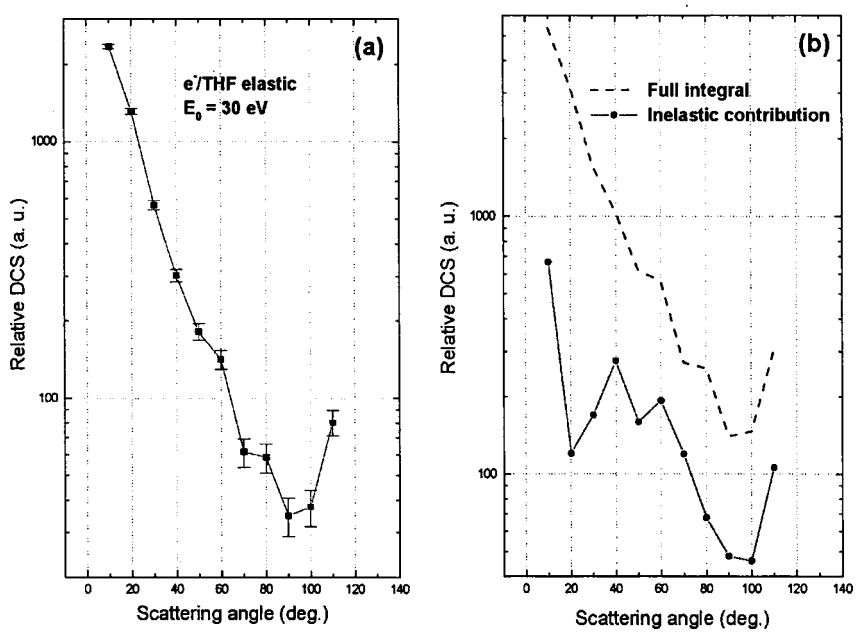

FIGURE 3. (a) Relative differential cross section for elastic electron scattering by THF molecule versus scattering angle at 30 eV impact energy (measured at the maximum of the peak). (b) Inelastic contribution to the integral signal in the range up to 0.45 eV of energy loss as a function of scattering angle at 30 eV impact energy.

Without the influence of inelastic scattering (related to the excitation of rotational and vibrational levels), and supposing the transmission function to be constant in this small energy region, the spectrum around zero energy loss (see figure 2) should be symmetrical. Hence, one can try to estimate the contribution of inelastic scattering (dominantly defined by vibrational excitations) according to the difference between left and right part of the spectrum. The influence of inelastic scattering up to 0.45 eV of electron energy loss to the integral signal, as a function of scattering angle, is presented in figure 3b. One can see the existence of the minimum at about 90°, as for the elastic DCS. However, it is interesting that inelastic angular dependence clearly

reaches the local maximum between 40° and 50°. This could be connected with the strong contribution of the shorter-ranged terms (e. g. polarization, ...), which is again important for the investigation of damage induced to DNA by secondary low-energy electrons [1, 2]. Such kind of behavior has been already observed earlier for other molecules [3, 4].

CONCLUSION

For the first time, the elastic electron scattering by tetrahydrofuran molecule (C_4H_8O) was investigated as a function of angle at fixed impact electron energies. This molecule is a DNA backbone sugar-like analogue and, hence, these results are of importance for the investigation of electron induced DNA damages. The relative DCS for elastic electron-THF scattering is presented for 30 eV impact energy as a function of scattering angle. Also, the contribution of inelastic scattering below 0.45 eV of energy loss was investigated as a function of angle. Further works will include similar measurements for more DNA backbone sugar-like analogues, such as THF derivates.

ACKNOWLEDGMENTS

This work was supported by European Cooperation in the field of Scientific and Technical Research, Action P9 – Radiation Damage in Biomolecular Systems. Part of the authors (A. M. and B. M.) are also grateful for the support of Ministry of Science, Environmental Protection of Republic of Serbia under project OI1424.

REFERENCES

1. Lepage M., Letarte S., Michaud M., Motte-Tollet F., Hubin-Franskin M.-J., Roy D., and Sanche L. , *J. Chem. Phys.* **109**, 5980-5986 (1998).
2. Antic D., Parenteau L., Lepage M., and Sanche L., *J. Phys. Chem. B* **103**, 6611-6619 (1999).
3. Motte-Tollet F., Hubin-Franskin M.-J., and Collin J. E., *J. Chem. Phys.* **97**, 7314 (1992)
4. Motte-Tollet F., Heinesch J., Gingell J. M., and Mason N. J., *J. Chem. Phys.* **106**, 5990-6000 (1997)
5. Trajmar S., Register D. F., and Chutjian A., *Phys. Rep.* **97(5)**, 219-356 (1983)

Differential Cross Section for Elastic Electron Scattering by Pb Atom

S. Milisavljević, M. Parđovska, D. Šević, V. Pejčev*, D. M. Filipović**, B. P. Marinković

Institute of Physics, P. O. Box 57, 11001 Belgrade, SCG
**Faculty of Natural Sciences, University of Kragujevac, Kragujevac, SCG*
***Faculty of Physics, University of Belgrade, P. O. Box 368, 11001 Belgrade, SCG*

Abstract. A crossed electron atom beam technique has been used to measure the differential cross sections (DCSs) for elastic electron scattering by Pb atom at electron impact energy (E_0) of 40 eV and within scattering angles (θ) from 10 to 148°. Our results are normalized and then compared with existing experimental data.

INTRODUCTION

In the Laboratory for Atomic Collision Processes of the Institute of Physics, Belgrade, we undertook a series of electron spectroscopic measurements to study electron collision with metal atoms such as Hg [1], Zn and Cd [2], Ca [3]. The last target used in our electron scattering experiment was Pb atom. Here we present the preliminary results for relative differential cross sections for elastic electron scattering by atomic lead at 40 eV at scattering angles between 10 and 148°.

EXPERIMENT

Electron spectrometer ESMA used in this experiment is designed for crossed electron atom beam measurements in which an atomic beam was perpendicularly crossed by monoenergetic electron beam and it has been described earlier [3].

Pb vapour beam has been produced by heating oven crucible containing Pb metal by two separate heaters [2]. Working temperature was about 900°C and background pressure was of the order of 10^{-5} Pa. The energy scale was calibrated by measuring the position of the feature in elastic scattering attributed to the threshold energy of the 6p7s ^{3}P state of Pb at 4.33 eV. The uncertainty of the energy scale was determined to be 100 meV, overal energy resolution 65 meV and the angular resolution was estimated to be 1.5°.

The scattered electron intensity at fixed electron impact energy E_0 = 40 eV and energy loss ΔE = 4.33 eV was measured as a function of scattering angle. Procedure of measurement included a few steps. Before each measurement the energy loss spectra were obtained. Then, scattering intensities were measured at small scattering angles

from -10° to +10° and the position of true zero angle was determined from the symmetry of these angular distributions.

An effective length correction factor [4] appropriate to our experimental conditions converted the measured signals to relative differential cross sections. These corrections were estimated on the basis of procedure described earlier [5].

RESULTS AND DISCUSSION

Obtained experimental results for relative differential cross sections for elastic electron scattering by Pb atom at E_0 = 40 eV impact energy are presented in figure 1.

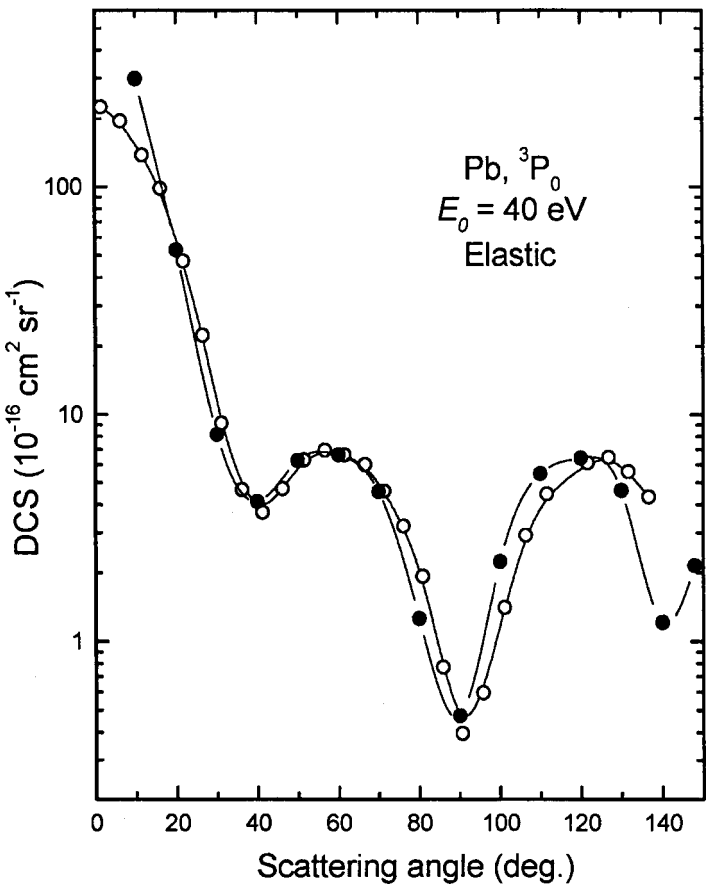

FIGURE 1. Differential cross section for elastic electron scattering by Pb atom at 40 eV impact energy: •, present results; ○, experimental results by Williams and Trajmar [6].

The relative DCSs were normalized at scattering angle of $\theta = 60^{\circ}$ to the experimental cross section by Williams and Trajmar [6]. As one can see, the shape of present angular distribution is in very good agreement with previous measurements [6]. We have covered broader angular range and we were able to obtain the third DCS minimum at around 140°.

We will extend our measurements to other impact energies and to the other states of Pb. These results, as well as absolute values for DCSs presented in this work which will be determine from inelastic to elastic intensity ratio at particular angle, we will present at the conference.

ACKNOWLEDGMENTS

This work has been carried out within project OI 1424 financed by MNZŽS of Republic Serbia.

REFERENCES

1. Panajotović, R., Pejčev, V., Konstantinović, M., Filipović, D., Bočvarski, V., and Marinković, B., *J. Phys. B: At. Mol. Opt. Phys.* **26**, 1005 (1993).
2. Predojević, B., Šević, D., Pejčev, V., Marinković, B. P., and Filipović, D. M., *J. Phys. B: At. Mol. Opt. Phys.* **36**, 2371 (2003).
3. Tošić, S., Šević, D., Pejčev, V., Filipović, D. M., and Marinković, B. P., Fifth General Conference of the Balkan Physical Union (BPU-5), Vrnjačka Banja, SCG, Avgust 25 – 29, 2003, Book of Abstracts, Eds. S. Jokić *et al*, p.54.
[http://www.phy.bg.ac.yu/~bpu5/proceedings/Papers/SO04%20-%20002.pdf]
2. Brinkman, R. T., and Trajmar, S., *J. Phys. E: Sci. Instrum.* **14**, 245 (1981).
5. Marinković, B., Pejčev. V., Filipović, D., and Vušković, L., *J. Phys. B: At. Mol. Opt. Phys.* **24**, 1817 (1991).
6. Williams, W., and Trajmar, S., *J. Phys. B: Atom. Molec. Phys.* **8**, L50 (1975).

Uniformity of the Magnetic Field of CTEM and Its Optimization

M. Parđovska, D. Šević, B. Marinković

Institute of Physics, P.O. Box 68, 11080 Belgrade, SCG

Abstract. In the cylindrical trochoidal monochromator the high-energy resolution electron beam is formed in the longitudinal magnetic field. In this paper we present numerical and experimental results of generating uniform magnetic field. First, we analyze system consisting of three coils. The system is realized in our laboratory. Then, we consider optimization of system with five coils, and the ideal system in which the windings of five coils would be positioned on the spherical surface. These simulations are done by C++ program.

INTRODUCTION

One basic requirement for studies in interaction of electrons with atoms and molecules is the production of electrons with well-defined properties, especially regarding energy and angular distribution. In our experiment we use trochoidal electron monohromator [1]. Crossed magnetic and electric fields in cylindrical symmetry are used to select the electrons [2,3].

The simplest system that produces a uniform magnetic field is Helmholtz pair system. For our purposes, the large range in which uniform magnetic field is required means an enormous radius of coils. Maxwell's three – coil combinations give a better results. In our experiment we use three coaxial coils. This paper presents dependence of uniformity of axial component of magnetic field when we change number of the turns in the coils and the intensity of current through coils. Our system generates a magnetic field more uniform than in the case of Helmholtz pair system. Generally, any system consisting of odd number of coils generates a magnetic field more uniform than system with even number of coils. The ideal system (to which all generating systems must compare) is that of a uniform field produced by a close, spherical current sheet or winding [4].

THE CASE OF THREE COILS

First of all, it is presented how varying of number of turns influence uniformity of magnetic field. The simulation takes into account physical dimensions of three-coil system used in our experiment [5]. The current of 1A was supplied to outer coils with 600 turns. We varied the number of Amper-turns of central coil. The results of simulations are shown in Figure 1.

Measured results of our realized three-coil system are in good agreement with results of simulations. The uniformity of measured magnetic field is the best when ratio between Amper-turns products of central and outer loops is 0.5585, as predicted by simulations.

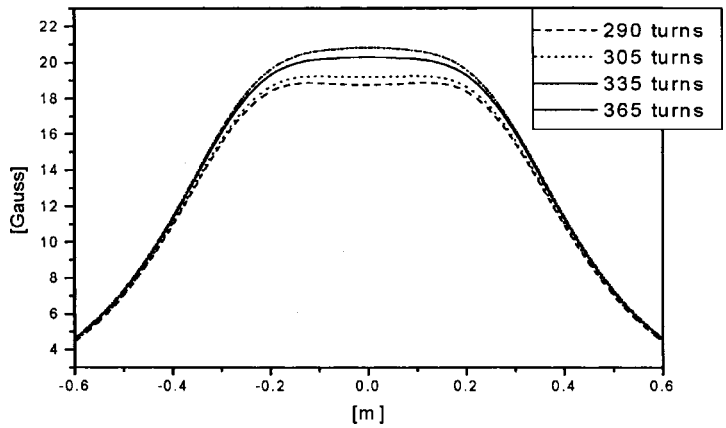

FIGURE 1. Three-coil system: dependence of axial component of the magnetic field on Amper-turns product of the central coil.

THE CASE OF FIVE COILS

The addition of two more coils near outers allows big improvement. This way, it is easier to solve the problem of heating of the windings. Two added coils are the same as the outer ones. They have 600 turns. Again, we varied the number of Amper-turns of the central coil. Simulation results are shown in Figure 2.

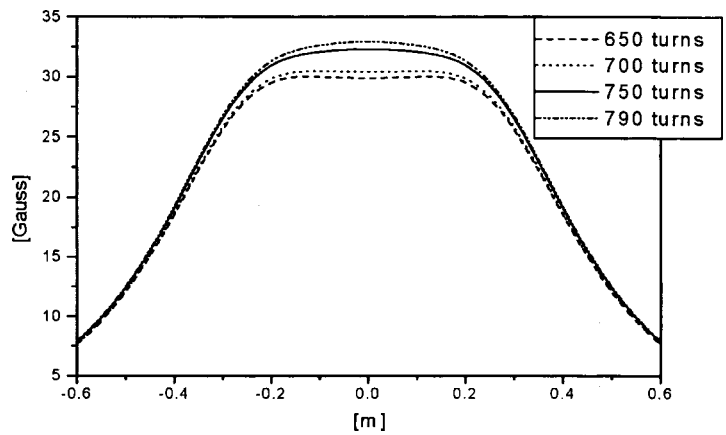

FIGURE 2. Five-coil system: dependence of axial component of the magnetic field on Amper-turns product of the central coil.

THE OPEN SPHERICAL CURRENT SHEET

Let us consider an open spherical current sheet of radius R, with axis z, whose opening is determined by the spherical angular coordinates θ_1 and θ_2. The surface current density **j** is assumed to have the following form:

$$j = j\varphi u\varphi , \quad j\varphi = - j0P11 (\cos \theta) = j0\sin\theta , \quad \theta 1 < \theta < \theta 2 , \qquad (1)$$

where j_0 is some constant having the dimensions of A/m. This current sheet can be constructed by winding a sphere of radius R, from θ_1 to θ_2, with a filament carrying a current I in such a way that the linear turn density along the axis N_z is constant; that is, the planes of the turns are equidistant along z. In that case the constant j_0 is $j_0 = N_z I$. When the spherical current sheet is completely closed ($\theta_1 = 0$, $\theta_2 = \pi$), the only no vanishing source constant is $h_1 = 2j_0/3$. For $r < R$, the magnetic field is constant through – out the sphere: $\mathbf{H} = h_1 \mathbf{u}_z$. For $r > R$, the magnetic field is that of a z- oriented dipole.

FIVE-COILS SYSTEM WITH WINDINGS POSITIONED ON A SPHERICAL SURFACE

We have also carried out numerical calculations by simulation for field system consisting of M = 5 parallel loops symmetrically placed with respect to the equatorial plane z = 0 on a spherical surface of radius R. All loops carry the same current I = 1 A circulating in the same direction. The M is odd, and one loop with total number of turns $N_0 = 720$ coincides with the equatorial circle and (M-1)/2 loops are located on either side of it. The distance to each other loop is 0.16m. Characteristics of coils are presented in table 1. Highly uniform magnetic field of about a 30 Gausses is obtained, as shown in Figure 3.

TABLE 1. Characteristics of the spherical five–coil system

	1	2	3	4	5
Radius [m]	0.205	0.310	0.386	0.310	0.250
Number of turns	450	550	720	550	450
Current [A]	1	1	1	1	1

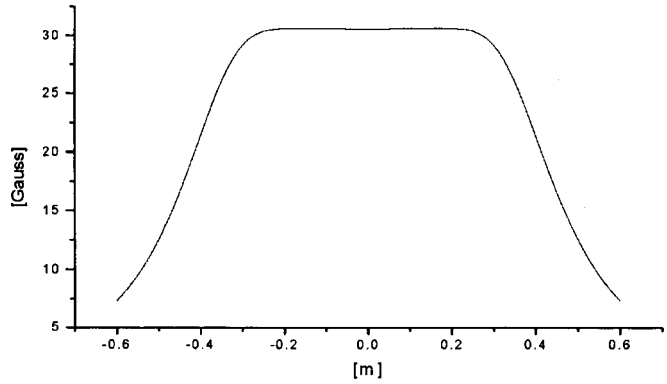

FIGURE 3. Axial component of the magnetic field of five-coils system with windings positioned on a spherical surface.

CONCLUSION

Simulation results for three-coil, five-coil and five-coil spherical magnetic field system are presented. Because five-coil system achieves needed intensity of magnetic field when supplied with lesser intensity of current, it offers the big improvement over three-coil system, regarding the heating of windings.

ACKNOWLEDGMENTS

This work has been carried out within project OI 1424 financed by MNZŽS of Republic Serbia and COST Action P9 RADAM.

REFERENCES

1. V.Grill, H.Drexel, W. Sailer, M. Lezius and T. D. Märk "*The working principle of the trochoidal electron monochromator revisited*", International Journal of Mass Spectrometry **205** (2001) 209 – 226.
2. M. I. Romanyuk, O. B. Shpenik *"Crossed – Field (trochoidal) electron monochromators and their optimization"*, Meas. Sci. Technol. **5** (1994) 239 – 246.
3. B. Marinković, Ping Wang, and Alan Gallagher, "*Threshold electron excitation of Na*" Phys. Rev. A **46** (1992) 2553 – 2557.
4. E. Boridy, *" Magnetic Fields Generated by axially symmetric systems*" J. Appl. Phys. **66**, No.12, (1989) 5691 – 5701.
5. M. Pardovska, D. Šević, B. Marinković, A. Milosavljević, S.Madžunkov *"Generator of Magnetic Field in Experiment SELE"*. XI Congress of Physicists of Serbia and Montenegro, June 3 – 5th, Petrovac na Moru, 2004, contribution [S2-13].

Correlation Between Radon Exhalation and Air Ion Concentration

P.M. Kolarž, B.P. Marinković, D.M. Filipović

Institute of Physics, Belgrade, Serbia and Montenegro, kolarz@phy.bg.ac.yu
Institute of Physics, Belgrade, Serbia and Montenegro, bratislav.marinkovic@phy.bg.ac.yu
Faculty of Physics, Belgrade, Serbia and Montenegro, filipovic@ff.bg.ac.yu

Abstract. To confirm influence of ^{222}Rn and other Rn isotopes on air ion concentration through air ions pair production, we have performed an in situ experiment. Negative air ion concentration was measured before and after stopping radon exhalation from the ground. Measuring of air ions was done using Gerdien type air ion detector constructed and built in Institute of Physics, Belgrade.

INTRODUCTION

Radon

Radon is the heaviest of noble gasses. His decaying products are ^{238}U, ^{232}Th or ^{235}U which occur naturally in the earth's crust. Three radon isotopes dominate in the nature: ^{222}Rn, ^{220}Rn (known as thoron) and ^{219}Rn (known as actinon). The half-lifes of this isotopes are: 3.8 *days* (^{222}Rn), 55.6 *s* (^{220}Rn) and 3.96 *s* (^{219}Rn) [1]. The α decay of ^{222}Rn with energy of 5.59 *MeV* is followed by a series of further decays. Final state of these decays is stable lead. ^{222}Rn progenies, i.e., the short-lived atoms into which ^{222}Rn decays, are isotopes ^{218}Po (187 *s*), ^{214}Pb (27 *min*), and ^{214}Bi (20 *min*). Polonium and bismuth also emit α particles with energies over 5 *MeV*, same as thoron and actinon. This radon daughter atoms also float around in the air, during short time of their existence, often becoming attached to dust particles.

The actual release of radon from the pore space in the ground or soil gas to ambient air is called exhalation. The rate of this process is a function of various parameters such as: radon concentration in soil gas, soil porosity and meteorological factors as precipitation and atmospheric pressure [2]. Duenas et al. [3], showed decreasing dependance of radon release with respect to soil humidity and explained it with reduction of soil porosity and consequently in a diminution of gas diffusion rates.

Further mixture of radon in ambient air is by diffusion. Since it is 7.5 times heavier than air, radon exists only in near ground levels where soil allow exhalation. When radon reaches the height of approximately 1 *m* above the soil surface, it's dispersion is determinated by atmospheric stability parameters. This stability is function of vertical

temperature gradient, direction and velocity of the wind and turbulence. Principally, radon concentration in atmospheric air decreases exponentially with altitude.

Small air ions

Small air ions, also called nanometric fast air ions, are one of basic constitutents of atmospheric air and main cause of atmospheric conductivity. Also, they are potential cause for aerosol generation and clouds formation through the specific processes of nucleus condensation. Their production in the atmosphere is a consequence of natural sources such as cosmic rays, natural radioactivity of the air and ground. This production varies with the height (fig.1) [4]. Near the ground radon decay products are major source of ionization, but with the height elevation, of about few hundred meters above earth surface, dominant source are cosmic rays.

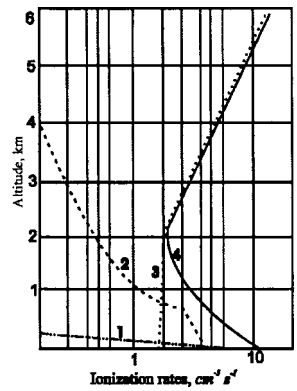

FIGURE 1. Various ionization rates from 0 to 6 km height: 1. from soil, 2. from radon, 3. from cosmic rays at 35° N, 4. total.

Small air ions are clustered central ions with 4-12 H_2O molecules, varying on their molecular structure polarity. Their typical concentration is 5×10^8 *ion/m*^{3} and average mobility is $\mu \geq 0.5\ 10^{-4}\ m^2V^{-1}s^{-1}$ in fair weather conditions, defined as: pressure p=1013 *mbar*, t=25 °*C*, cloudiness less than 3/10 and wind slower than 5 *m/s* [5] and in unpolluted air.

INSTRUMENTATION

Detection of air ions is possible by using their electrical properties. In 1905. Gerdien developed instrument for atmospheric ion measurements known as "Gerdien condenser" at present [6]. A new designed, Gerdien-tipe, detector was made in our laboratory in the Institute of Physics, named Cylindrical Detector of Ions - 07 (CDI-07). This instrument could be applyed for small air ion concentration determination and also for air conductivity measurements.

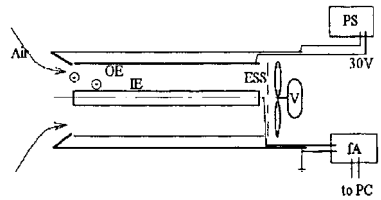

FIGURE 2. Air ion detection method (OE – outside electrode, IE – central electrode, ESS – electrostatic shield, PS – power supply, fA – femptoampermeter, PC – personal computer).

Ions from ambient air are aspirated in condenser by fan and voltage applied between the outer and central electrode causes ions of the same sign as the voltage, to be repelled from the outer electrode to the central. If the threshold potential is high enough, all fast nanometric ions of corresponding polarity will be collected on the central electrode and they cause a small current. Ions of the opposite sign are attracted by the outer electrode and neutralized. Small current from central electrode passes through 1 GΩ resistor and operational amplifier AD549L magnifies small voltage signal from the resistor to the potential signal, convenient for further processing. If air flows through the tube then a continual current can be recorded, which is directly proportional to the number concentration of small ions in the air (eq.1)[7].

$$I = qnv\pi\left(R_o^2 - R_i^2\right) \tag{1}$$

where q is ion charge, n ion concentration, v air velocity along the axis, R_o radius of the outer electrode and R_i radius of the central electrode.

EXPERIMENTS

Experiments were done several times on different places with similar results and one given belove was held at Kalemegdan park, Belgrade, on terrain that is assumed to be porous and addicted for radon exhalation. Measuring was done on 0.6 m above the ground surface during fine weather conditions. Since releasing of ^{222}Rn in ambient air is also function of temperature measuring place was chosen to be in shadow.

The experiment was performed in two steps. First, measuring of negative small air ion concentration above dry ground and then repeating measuring after watering. Stopping of radon exhalation was done by quick and capasious watering about 10 m^2 around the measuring place.

RESULTS AND DISCUSSION

The results showed that ion concentration is approximately 2.5 times smaller after the soil watering (fig. 1). This effect is remarkable despite it is known that negative air ion concentration is increasing function of relative humidity [8]. Since lifetime of ions in clean air is about few minutes, ion concentration after effusion could be refer to cosmic rays ionisation processes and residual air radioactivity.

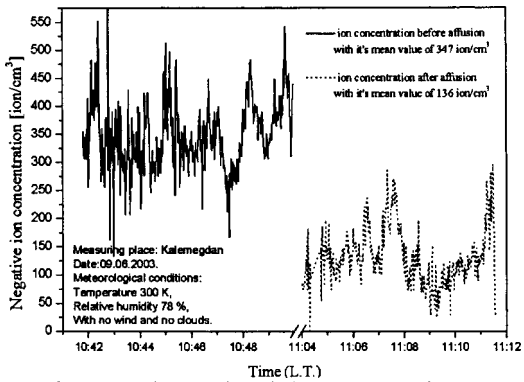

FIGURE 3. Decrease of nanometric negative air-ions (0.36 - 1.6 nm) concentration after stopping of radon exhalation from the ground.

This phenomenon could be explained with sudden stopping of radon isotopes exhalation from the ground. Ion pairs formation induced by ionizing radiation of ^{220}Rn and ^{219}Rn is short living so as the result, negative ion concentration decreases.

^{222}Rn in the air decays within a few days but his relatively short half-life daughters decay faster. In that way three α particles, one by radon and two by it's daughters take part in radon-induced ionization processes, so stopping of radon exhalation induces significant drop in air ionization. On higher elevation this effect is less significant and more dependant on meteorological parameters.

ACKNOWLEDGMENTS

This work has been done under project OI 1424 financed by MNZŽS of Republic of Serbia.

REFERENCES

1. Friedman, H., 1997, Radon - the Fleeting Daughter of Radium, Nuclear Physics News, 7,14.
2. WHO, 1983 elected radionuclides. Environmental Health Criteria 25. Geneva: World Health Organization.
3. Duenas, C., Fernandez, M.C., Carretero, J., Liger, E., Perez, M., 1997, Release of ^{222}Rn from some soils, Ann. Geophysicae 15, 124 - 133.
4. Mohnen, V.,1977, Formation, nature, and mobility of ions of Atmospheric importance, Book of contributed papers of the Electrical Processes in Atmospheres, Darmstadt.
5. Dolezalek, H., 1982, Atmospheric electricity. In: Handbook of Chemistry and Physics, (Ed.) R.C. Weast, CRC Press, Inc. Boca Raton.
6. Gerdien, H., 1905, Demonstration eines Apparates zur Apsoluten Messung der elektrischen Leitfahigheit der Luft, Phys.Z. 6, 800-1.
7. Chalmers, A., 1967, Atmospheric electricity, 2nd edition, Pergamon Oxford.
8. P. Kolarž, J. Šekarić, B.P. Marinković and D.M. Filipović, 2004, Correlation between some of meteorological parameters measured during the partial solar eclipse, 11th August 1999, submitted to J. Atm. and Sol-Ter Phys.

The Simulation of Two-Dimensional Detector for Metastable Rare Gas Atoms

A. Milosavljević[1], V. Bočvarski[1], B. P. Marinković[1], F. Perales[2], J. Robert[2], J. Baudon[2], J.-C. Karam[2]

[1]*Institute of Physics, PO Box 68, 11080, Belgrade, Serbia and Montenegro*
[2]*Laboratoire de Physique des Lasers, Université Paris 13, 93430-Villetaneuse, France*

Abstract. Two-dimensional detector with high spatial and temporal resolution for metastable rare gas atoms was analyzed by electron ray tracing program Focusing voltage and magnification were determined for the given geometry and the influence of different parameters was examined. A new design of 2D-detector with variable magnification is proposed.

INTRODUCTION

Recently, Kurtsiefer and Mlynek [1] have presented a 2-dimensional detector with high spatial and temporal resolution for metastable rare gas atoms. Their approach involved a detection technique where the conversion process from metastable atom to the first electron was separated from the electron avalanche process. By using electron imaging techniques, the conversion plane could be magnified to get better spatial resolution.

The imaging was done by using a set of electrostatic tube lenses shown in figure 1. It was analytically described according to approximate algebraic expressions and the realized experimental set-up was tested. The diameter of the extraction hole is 1.5 mm, while the lens diameters are 5 mm and 10 mm. The separation of the conversion electrode E_1 and the first electrode E_2 was chosen to be 5 mm.

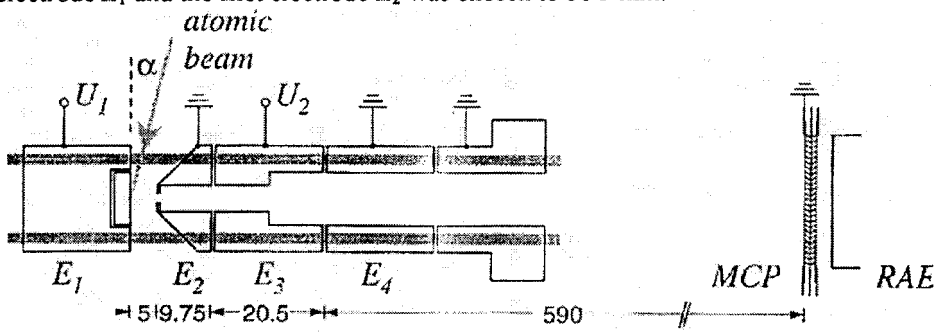

FIGURE 1. Experimental set-up of atom detector by Kurtsiefer and Mlynek [1]. The system is designed for magnification of 16, with extraction voltage U_1 = 15 kV. The focus onto a multi-channel plate array (MCP) and consecutive resistive area element (RAE) was calculated to be reached at U_2 = 9.85 kV, while it was experimentally obtained for 10.06 kV.

PRESENT MODEL

The SIMION [2] model of the low magnification electron-optical system of Kurtsiefer and Mlynek [1] is presented in figure 2. Additional programming was used for continual changing of starting parameters and lens potentials. The parameters (elevation angle and radius) of simulated electron trajectories were collected at L_{col} = 89 mm from the conversion plane, far from the influence of lens fields. After having passed the lenses, electron trajectories should be linear, so it is easy to calculate the spatial electron distribution at the detection plane.

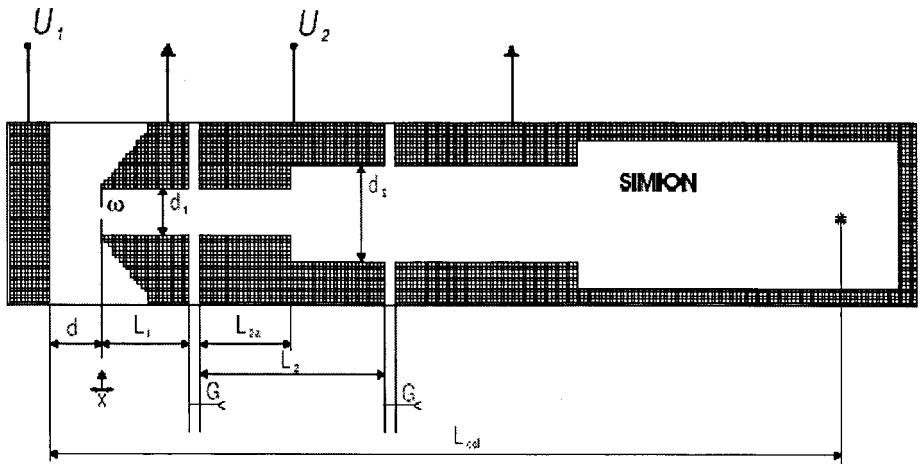

FIGURE 2. Present SIMION model of the set-up for atom detector. The detection plane is omitted in order to obtain more accurate lens characteristics. Most of calculations were performed with the following parameters: d = 5 mm, x = 0.5 mm, L_1 = 9.7 mm, L_2 = 20.4 mm (L_{2a} = 10.2 mm), G = 0.9 mm ω = 1.4 mm, d_1 = 5 mm, d_2 = 10 mm. The detection plane was assumed to be at X_{det} = 625.25 mm.

Influence of different parameters to the focusing voltage

The focusing voltage for the given parameters was found to be 9.68 kV. That is in some disagreement with theory (9.85 kV) and experiment (10.05 kV) found by Kurtsiefer and Mlynek [1]. Influence of different parameters to the focusing voltage is therefore closer investigated. It is found that the change of about 0.5 mm of the distance between conversion plane and extraction plane causes the shift of focusing voltage within 0.1 kV. Influence of focusing electrode length L_2 and gap between electrodes G is presented in figure 3. The later factor (G) seems to be more important. Also, it was investigated the influence of the distance of metastable atom conversion place from the conversion plane (X_0) as well as influence of distance between conversion plane and detector. By changing the width of the extraction hole from 0.5 mm to 1.5 mm we did not find any influence on focusing voltage. A slight influence of starting electron energy (typically considered to be 10 eV) was found in the investigated range from 6 eV to 14 eV.

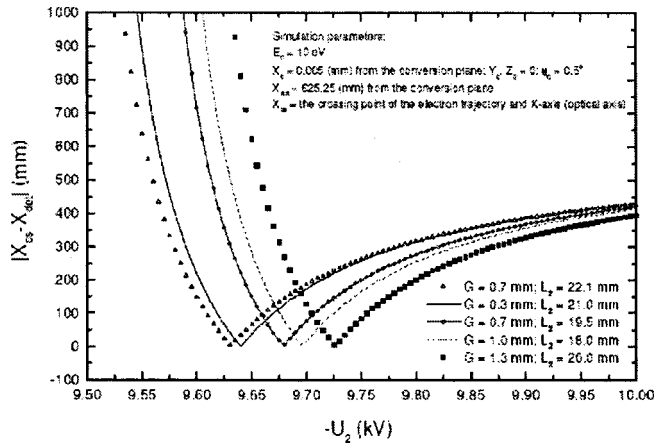

FIGURE 3. Influence of focusing electrode length L_2 and gap between electrodes G.

Angular and energy spread of starting electrons

The simulation of imaging of one – central point on the conversion plane onto detector plane, as a function of focusing voltage U_2 is presented in figure 4. Owing to both energy spread of 10 eV (5 eV to 15 eV) and angular spread of $\pm 90^0$ of starting electrons, the single point is imaged onto detector plane with some Y distribution, which depends on focusing voltage. The focus is confirmed to be at 9.68 kV.

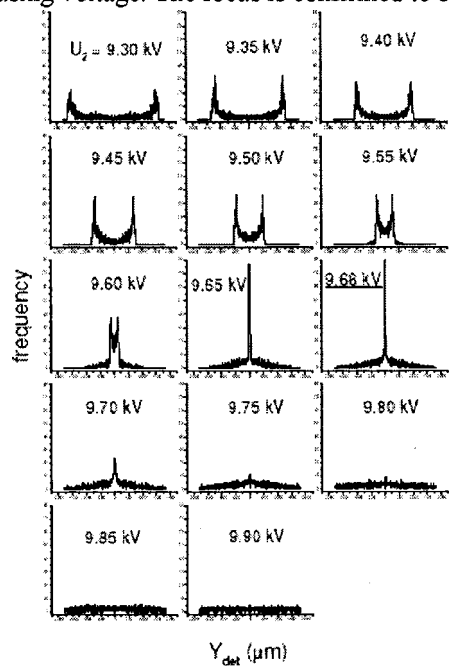

FIGURE 4. The image of the central point versus focusing voltage.

IMPROVED MODEL

Improved model of electron imaging system with variable magnification for 2D – detector with high spatial resolution for metastable gas atoms is presented the same authors elsewhere [3]. The magnification is regulated by appropriate choice of lens potentials only, using two electron imaging stages. In the first one, the electrons are extracted from the conversion plane and imaged to an intermediate real image with a four-electrode unipotential zoom lens. At the second stage, the real intermediate image is projected onto the detection plane with the use of three-electrode einzel lens. Continual tuning of magnification in the range of 14 to over 55 is obtained even with smaller longitudinal size of the detector (about 500 mm).

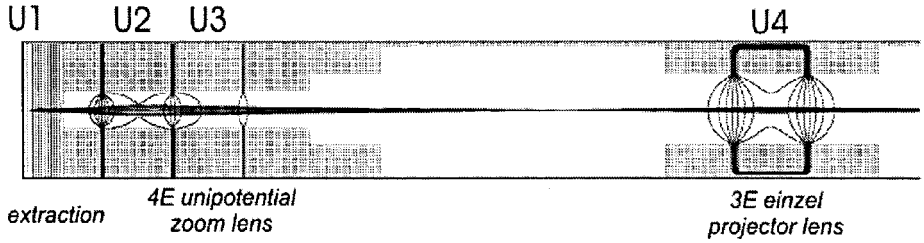

FIGURE 5. Setup of improved electron-optical system.

CONCLUSION

A 2-dimensional detector with high spatial and temporal resolution for metastable rare gas atoms was analyzed by SIMION electron ray tracing program. For the given geometry, focusing voltage was determined and the influences of different parameters on its value were examined. Owing to both energy and angular spreads of starting electrons, the strong dependence of imaging the single point at detector plane versus focusing voltage was found. An improved model with variable magnification is proposed.

ACKNOWLEDGMENTS

This work has been carried out within project OI 1424 financed by MNZŽS of Republic Serbia and under bilateral France – Serbia programm "Pavle Savić".

REFERENCES

1. Kurtsiefer, Ch., and Mlynek, *Appl. Phys. B* **64**, 85-90 (1997).
2. Dahl, D. A., *SIMION 3D VERSION 6.0, User's Manual*, (1995).
3. Milosavljević, A., Bočvarski, V., Marinković, B. P. Perales, F., Robert, J., Baudon, J., and Karam, J.-C., "The Electron Imaging System With Variable Magnification For A 2d Detector With High Spatial Resolution For Metastable Gas Atoms" in *European Conference on Atomic and Molecular Physics –ECAMP8 – 2004*, edited by N. J. Mason et al., Europhysics Conference Proceedings, 2004.

CIP – Каталогизација у публикацији
Народна библиотека Србије, Београд

537.56(082)
539.186.2(082)
539.121.7(082)
533.9(082)

SUMMER School and International Symposium
on the Physics of Ionized Gases (22 ; 2004 ; Bajina Bašta)
Contributed Papers and Abstracts of Invited Lectures,
Topical Invited Lectures and Progress Reports / 22nd Summer
School and International Symposium on the Physics of
Ionized Gases SPIG 2004 [23. – 27. August 2004, Bajina Bašta]
; editor Ljupčo Hadžievski. – Belgrade : Vinča Institute of
Nuclear Sciences, 2004 (Belgrade : Branmil). – XIX, 592 str. :
graf. prikazi, tabele ; 24 cm

Tiraž: 300. – Str. III: Preface / Ljupčo Hadžievski.
– Bibliografija uz svaki rad. – Registar.

ISBN 86-7306-063-6
1. Hadžievski, Ljupčo
а) Гасови, јонизовани – Зборници б) Атоми – Елементарне
честице – Интеракција – Зборници ц) Плазма - Зборници
COBISS.SR-ID 115737612